Journal of Applied Polymer Science

Biobased Thermosetting Resins Composed of Terpene and Bismaleimide

Mitsuhiro Shibata, Masanori Asano
Department of Life and Environmental Sciences, Faculty of Engineering, Chiba Institute of Technology, 2-17-1, Tsudanuma, Narashino, Chiba 275-0016, Japan
Correspondence to: M. Shibata (E-mail: shibata@sky.it-chiba.ac.jp)

ABSTRACT: Prepolymers prepared by reactions of 1,1′-(methylenedi-4,1-phenylene)bismaleimide (BMI) with myrcene (Myr) and limonene (Lim) in 1,3-dimethyl-2-imidazolidinone (DMI) at 150°C were compressed at 250°C to produce crosslinked Myr/BMI [molar ratio = 2:2–2:5 (MB22–MB25)] and Lim/BMI [molar ratio = 1:1 (LB11)] resins. The ^{1}H-NMR analysis of the model reaction products of Lim and Myr with *N*-phenyl maleimide (PMI) in DMI at 150°C revealed that a Diels–Alder reaction for Myr/PMI and a vinyl copolymerization for Lim/PMI preferentially proceeded in addition to the occurrence of the ene reaction to some extent. The Fourier transform infrared data of the cured resins were consistent with the results of the model reactions. All of the cured resins, except for MB22, showed tan δ peak values and 10% weight loss temperatures that were higher than 330 and 440°C, respectively. The flexural strength and modulus values of the MBs were higher than those of LB11. Field emission scanning electron microscopy analysis revealed that MB22–MB24 were homogeneous, whereas some combined particles appeared in LB11. © 2012 Wiley Periodicals, Inc. J. Appl. Polym. Sci. 129: 301–309, 2013

KEYWORDS: biopolymers and renewable polymers; crosslinking; polyimides; properties and characterization; thermosets

Received 4 May 2012; accepted 18 August 2012; published online 9 November 2012
DOI: 10.1002/app.38477

INTRODUCTION

Biobased polymer products derived from annually renewable agricultural and biomass feedstock have become increasingly important as sustainable and eco-efficient products that can replace the products based exclusively on petroleum feedstock.[1–7] There are two approaches for preparing biobased polymers, in which (1) biomass resources are converted to monomers or key intermediates via large-scale biochemical processes (i.e., they are biorefined), and (2) biomass resources are directly used as ingredients in polymer synthesis.[8–10] To develop biobased thermosetting resins with various kinds of small-quantity production, it is important to directly use the specific or complicated structures originating from natural products.[11] Petroleum-based thermosetting bismaleimide resins are used as matrix resins for multilayer printed circuit boards and advanced composite materials in aerospace applications.[12–16] The improvement of water-resistant and low dielectric properties is required, especially for the application of thermosetting bismaleimide resins to electric materials. As a biobased component compounded with bismaleimide, which is a strong electrophile, the utilization of biomass resources with conjugated polyene and/or allylic moieties is effective because their functional group can undergo Diels–Alder and ene reactions, respectively. We already reported biobased bismaleimide resins composed of 1,1′-(methylenedi-4,1-phenylene)bismaleimide (BMI) and drying vegetable oils, such as dehydrated castor oil and tung oil.[17,18] To improve their thermal and mechanical properties, a natural polyene substance without a long aliphatic chain is desirable. Myrcene [Myr; 7-methyl-3-methene-1,6-octadiene (β-Myr)] is a monoterpene that has both conjugated diene and substituted allylic moieties. Myr is a component of essential oils of several plants, including laurel, wild thyme, and Myrcia. Myr is commercially prepared by the cracking of β-pinene (which has an annual worldwide production of 26,000 tons),[19] which is obtained from turpentine oil and can react with different dienophiles to give rise to a variety of fragrant compounds or their intermediates.[20–22]

In this study, biobased thermosetting resins were prepared by the reaction of BMI with Myr, and their thermal, mechanical, and water-resistance properties were investigated and compared with those of cured products of BMI and L-limonene (Lim). Lim is also a monoterpene, which is derived from mint oil. Lim does not have a conjugated diene moiety, which can undergo a Diels–Alder reaction with BMI. It was reported that the isopropylidene moiety of Lim and D-Lim (with an 1991 annual worldwide production of 50,000 tons)[19] undergoes radical polymerization with maleic anhydride and *N*-phenylmaleimide (PMI),

respectively.[23,24] To clarify the curing mechanism of BMI with Myr and Lim, an ^{1}H-NMR analysis of the reaction products of PMI with Myr and Lim was performed.

EXPERIMENTAL

Materials

Myr was supplied from Sigma-Aldrich Japan Corp. (Tokyo, Japan). Lim was supplied from Kanto Chemical Co., Inc. (Tokyo, Japan). PMI, BMI, triphenyl phosphine (TPP), and 1,3-dimethyl-2-imidazolidinone (DMI) were supplied from Tokyo Kasei Kogyo Co., Ltd. (Tokyo, Japan).

Model Reaction of Lim and PMI

A mixture of Lim (1.42 g, 10.4 mmol) and PMI (3.60 g, 20.8 mmol) in 5 mL of DMI was stirred at 150°C for 24 h. After the reaction, the mixture was poured into excess water, and the obtained precipitate was collected by filtration, washed with deionized water, and dried at 60°C in a vacuum oven to give a Lim/PMI reaction product (2.1 g) with a molar ratio of 1:2 as a yellow powder in 42% yield. The obtained product was abbreviated as TP12.

Model Reaction of Myr and PMI

A mixture of Myr (1.42 g, 10.4 mmol) and PMI (3.60 g, 20.8 mmol) in 5 mL of DMI was stirred at 150°C for 24 h. After the reaction, the mixture was poured into excess water, and the obtained precipitate was collected by filtration, washed with deionized water, and dried at 60°C in a vacuum oven to give a Myr/PMI reaction product (3.6 g) in a molar ratio of 1:2 as a yellow powder in 72% yield. The obtained product was abbreviated as MP12. The MP12 (1.20 g) was washed with methanol several times to wash out the produced Diels–Alder adduct and dried at 60°C in a vacuum oven to give an MP12 washed with methanol (0.50 g) in 42% yield. The MP12 washed with methanol was abbreviated as MP12m.

Curing Reaction of Lim and BMI

A mixture of Lim (4.13 g, 30.3 mmol), BMI (10.9 g, 30.3 mmol), and TPP (0.109 g, 1:100 weight ratio to BMI) in 15 mL of DMI was stirred at 150°C for 4 h. After the reaction, the mixture was poured into excess water, and the obtained precipitate was collected by filtration, washed with methanol, and dried at 60°C in a vacuum oven to give a Lim/BMI prepolymer (11.1 g) as a yellow powder in 74% yield. The prepolymer was compressed at 180°C and 5 MPa for 1 h and was subsequently compressed at 250°C and 5 MPa for 5 h to give a Lim/1,1′-(methylenedi-4,1-phenylene)bismaleimide cured resin (C-BMI) in a molar ratio of 1:1. The obtained cured resin was abbreviated as LB11. TPP was added as a catalyst for the homopolymerization of excess BMI because it was supposed from the results of the model reaction of Lim and PMI at a molar ratio of 1:2 that considerable amounts of maleimide group would remain. For comparison, a mixture of BMI 15.0 g (41.9 mmol) and TPP 0.15 g (1:100 weight ratio to BMI) was prepolymerized at 180°C for 1 h and was subsequently compressed at 250°C and 5 MPa for 5 h to give C-BMI.

Curing Reaction of Myr and BMI

A mixture of Myr (3.00 g, 22.0 mmol), BMI (11.8 g, 33.0 mmol), and TPP (0.118 g, 1:100 weight ratio to BMI) in 15 mL of DMI was stirred at 150°C for 4 h. After the reaction mixture was poured into excess water, the obtained precipitate was collected by filtration, washed with methanol, and dried at 65°C in a vacuum oven to give a Myr/BMI prepolymer (13.2 g) as a yellow powder in 89% yield. The prepolymer was compressed at 180°C and 5 MPa for 1 h and was subsequently compressed at 250°C and 5 MPa for 5 h to give Myr/C-BMI in a molar ratio of 2:3. The obtained cured resin was abbreviated as MB23. In a similar manner to the preparation of MB23, MB24 and MB25 were prepared in 84 and 77% yields, respectively. A similar reaction was performed without TPP only for a mixture of Myr 4.13 g (30.3 mmol) and BMI 10.9 g (30.3 mmol) to produce MB22 (13.4 g) in 89% yield because we supposed from the result of the model reaction of Myr and PMI at a molar ratio of 1:2 that the amount of remaining maleimide groups would be small.

Measurements

^{1}H-NMR spectra were recorded on a Bruker AV-400 (400 MHz, Madison, WI) with $CDCl_3$ as a solvent. Fourier transform infrared (FTIR) spectra were measured on an FTIR 8100 spectrometer (Shimadzu Co., Ltd., Kyoto, Japan) by the KBr method for the cured resins and the attenuated total reflectance method for Lim and Myr. The 10% weight loss temperature was measured on a thermogravimetric analyzer (TGA-50, Shimadzu) in a nitrogen atmosphere at a heating rate of 20°C/min. Dynamic mechanical analysis (DMA) of the rectangular plates (length = 40 mm, width = 6 mm, and thickness = 2 mm) was performed on a Rheolograph Solid (Toyo Seiki Co., Ltd., Tokyo, Japan) with a chuck distance of 20 mm, a frequency of 1 Hz, and a heating rate of 2°C/min on the basis of ISO 6721-4:1994 ("Plastics-Determination of Dynamic Mechanical Properties, Part 4:Tensile Vibration–Non-Resonance Method"). Flexural tests of the rectangular plates (length = 55 mm, width = 10 mm, and thickness = 2 mm) were performed at 25°C with an Autograph AG-I (Shimadzu). The span length was 30 mm, and the testing speed was 10 mm/min. Five composite specimens were tested for each set of samples, and the mean value was calculated. The morphology of the cured resins was observed by field emission scanning electron microscopy (FE-SEM) with a Hitachi S-4700 machine (Hitachi High-Technologies Corp., Tokyo, Japan). All samples were fractured after immersion in liquid nitrogen for about 30 min. The fracture surfaces were sputter-coated with gold to provide enhanced conductivity. The water absorption test of the cured resins was performed by measurement of the weight change after specimens with a size of 10 × 10 × 2 mm^3 were immersed in deionized water at room temperature for 24 h. Three specimens were tested for each set of samples, and the mean value was calculated.

RESULTS AND DISCUSSION

Characterization of the Model Reaction Product of Terpene and PMI

The model reaction of Lim/PMI at a molar ratio of 1:2 in DMI at 150°C for 24 h produced LP12. Figure 1 shows the ^{1}H-NMR spectra of Lim and LP12 in $CDCl_3$. The olefinic ^{1}H signals of the cyclohexene and isopropylidene moieties of Lim were observed at 5.44 ppm (s, 1H, H_a) and 4.76 ppm (s, 2H, H_b),

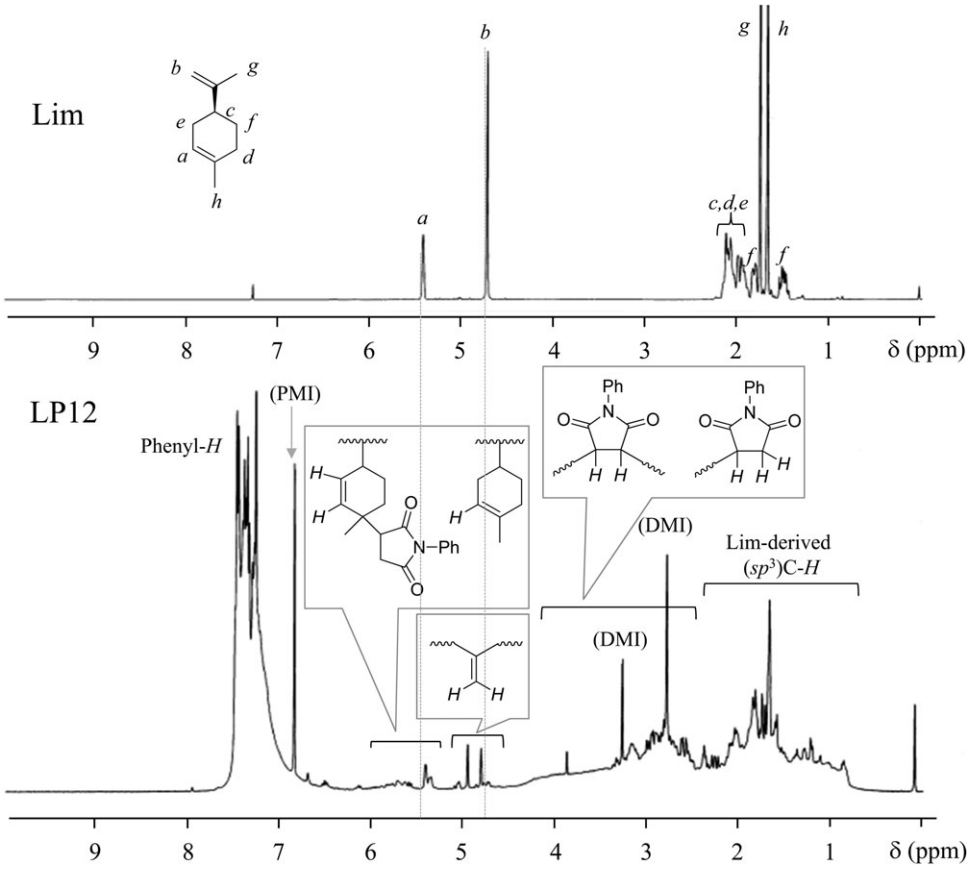

Figure 1. ^{1}H-NMR spectra of Lim and LP12 in $CDCl_3$.

respectively. The aliphatic ^{1}H signals of Lim were observed at 2.25–1.89 ppm (m, 5H, $H_{c,d,e}$), 1.84 (m, 1H, H_f), 1.78 ppm (s, 3H, H_g), 1.69 ppm (s, 3H, H_h), and 1.52 ppm (m, 1H, H_f). For LP12, the aliphatic ^{1}H signals increased at 4.4–0.8 ppm, and the olefinic ^{1}H signals decreased at 6.2–4.7 ppm relative to those of Lim; this suggested the preferential occurrence of the vinyl copolymerization of Lim and PMI. The fact that the olefinic proton signal at 4.70 ppm observed for Lim disappeared for LP12 suggested that the vinyl copolymerization with PMI occurred at the isopropylidene moiety of Lim. This result was in agreement with the previously reported results of a radical copolymerization of D-Lim and PMI at 60°C in the presence of 2,2′-azobisisobutyronitrile.[24] This was also reasonable because the reactivity of the radical polymerization of α,α-dialkyl substituted olefin is much higher than that of α,α,β-trialkyl substituted olefin. The fact that broad olefinic ^{1}H signals at 6.0–5.3 ppm were observed in addition to the ^{1}H signal at 5.40 ppm, corresponding to the H_a of Lim, indicated the formation of new cyclohexene moieties due to the ene reaction of the cyclohexene moieties of Lim and PMI. Also, the appearance of two olefinic ^{1}H signals at 4.97 and 4.82 ppm near the ^{1}H signal at 4.70 ppm, corresponding to the H_b of Lim, suggested the formation of a new >C=CH_2 moiety due to the ene reaction. A probable reaction mechanism of Lim and PMI based on these results is shown in Figure 2. First, the radical copolymerization of the isopropylidene moiety of Lim and the maleimide group of PMI was preferred, and subsequently, the ene reaction of the cyclohexene moiety of the copolymer and PMI proceeded to form new succinimide-substituted cyclohexene and methylene cyclohexane moieties. Although the radical polymerization was estimated to be preferred for the isopropylidene moiety of Lim, there was a possibility that the ene reaction with PMI occurred at the isopropylidene moiety, and subsequently, radical copolymerization with PMI occurred at the new succinimide-substituted isopropylidene moiety.[25,26]

On the other hand, the reaction of Myr/PMI in a molar ratio of 1:2 in DMI at 150°C for 24 h produced MP12. Figure 3 shows the ^{1}H-NMR spectra of Myr and MP12. Myr showed ^{1}H signals at 6.40 ppm (dd, 1H, H_a), 5.25 ppm (d, 1H, H_b), 5.16 ppm (t, 1H, H_c), 5.04 ppm (d, 1H, H_d), 5.00 ppm (s, 1H, H_e), 2.23–2.05 ppm (m, 4H, H_f), 1.73 ppm (s, 3H, H_g), and 1.63 ppm (s, 3H, H_h), and this was in agreement with the reported assignment of Myr.[27] The NMR spectrum of MP12 suggested that MP12 was mainly composed of the Diels–Alder adduct of 1:1 Myr/PMI and unreacted PMI. Thus, the Diels–Alder adduct showed ^{1}H signals at 7.52–7.22 ppm (m, phenyl-*H*), 5.66 ppm (s, 1H, H_l), 5.07 ppm (s, 1H, H_m), 3.25 ppm (m, 2H, H_n), 2.73–1.95 ppm (m, 8H $H_{o,p}$), 1.69 ppm (s, 3H, H_q), and 1.61 ppm (s, 3H, H_r). The ^{1}H signal of the maleimide group of PMI was observed at 6.84 ppm (s, 2H). In addition to their ^{1}H signals, weak and broad signals were observed at the chemical shift region lower than 5.3 ppm. To clarify their minor signals, the

Applied Polymer SCIENCE

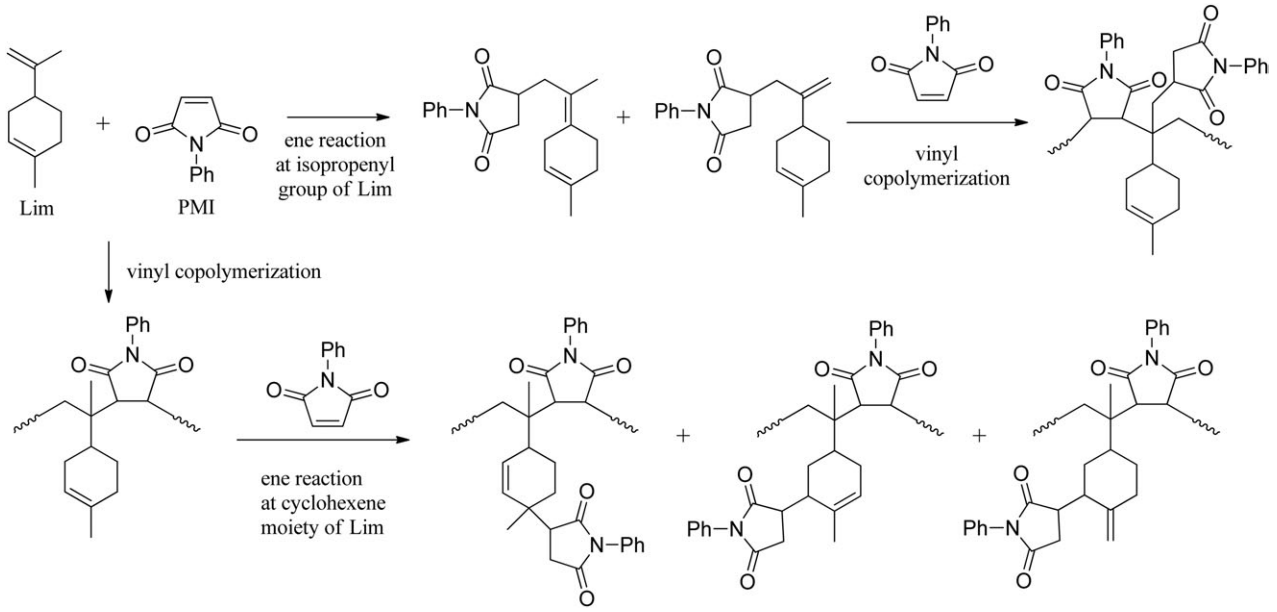

Figure 2. Probable reaction scheme of Lim and PMI.

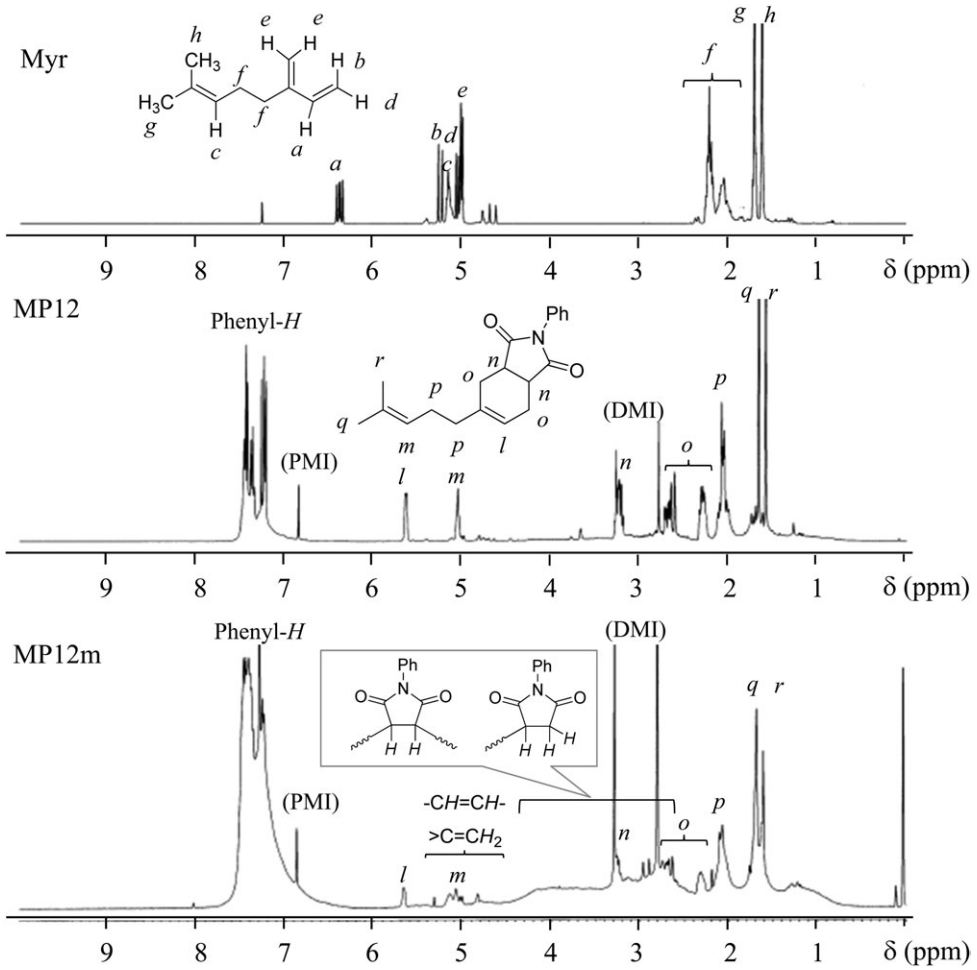

Figure 3. ^{1}H-NMR spectra of Myr, MP12, and MP12m in $CDCl_3$.

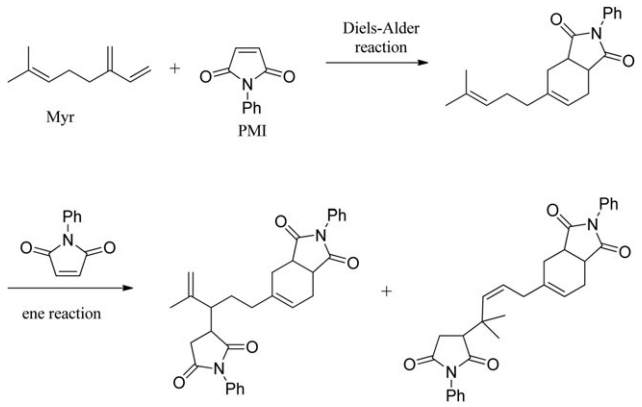

Figure 4. Probable reaction scheme of Myr and PMI.

Diels–Alder adduct contained in MP12 was removed by methanol washing. The obtained MP12m showed olefinic ^{1}H signals at 5.3–4.8 ppm and aliphatic ^{1}H signals at 4.3–0.8 ppm; this suggested the occurrence of the ene reaction with PMI at the isobutylene moiety of the Diels–Alder adduct. From these results, the probable reaction scheme of 1:2 Myr/PMI is shown in Figure 4. The Diels–Alder reaction between the conjugated diene moiety of Myr and the maleimide group of PMI occurred, and subsequently, the ene reaction with PMI at the isobutylene moiety of the Diels–Alder adduct proceeded to produce succinimide-substituted alkenes. There was a possibility that the formed alkenyl moiety further underwent the ene reaction and/or vinyl copolymerization with PMI.[25,26]

Characterization of the Cured Resin of Terpene and BMI

Powders of the Lim/BMI and Myr/BMI prepolymers prepared at 150°C for 4 h in DMI were finally compressed at 250°C for 5 h to produce LB11 and MB22–MB25. As revealed in the analysis of the model reaction at 150°C in DMI, we supposed that the vinyl copolymerization and Diels–Alder reactions were preferred for the prepolymers of Lim/BMI and Myr/BMI, respectively. Because the cured LB11 and MB22–MB25 were insoluble in general organic solvents, the reaction was analyzed by the FTIR method. The analysis of the C—H out-of-plane bending absorptions of alkenes was effective for identifying their substitution manner and cis–trans isomerism. For example, it is known that vinylidene $R_2C{=}CH_2$, *cis*-disubstituted RHC=CHR, *trans*-disubstituted RHC=CRH, and trisubstituted $R_2C{=}CHR$ show absorption peaks at 895–885 cm^{-1} (strong), 730–665 cm^{-1} (strong), 980–960 cm^{-1} (strong), and 840–790 cm^{-1} (medium), respectively.[28] It is also known that vinyl $RHC{=}CH_2$ shows absorption peaks at 995–985 cm^{-1} (strong) and 915–905 cm^{-1} (strong).[28] Figure 5 shows the FTIR spectrum of LB11 compared with those of Lim and BMI. The C—H out-of-plane bending absorption of the isopropylidene $R_2C{=}CH_2$ moiety of Lim at 887 cm^{-1} disappeared for LB11. The C—H out-of-plane bending absorption of the cyclohexene $R_2C{=}CHR$ moiety of Lim at 798 cm^{-1} remained in the spectrum of LB11, and new broad peaks were observed around 850–740 cm^{-1}. These results support the fact that vinyl copolymerization and a subsequent ene reaction occurred for LB11 in a similar manner to the reactions of LP12.

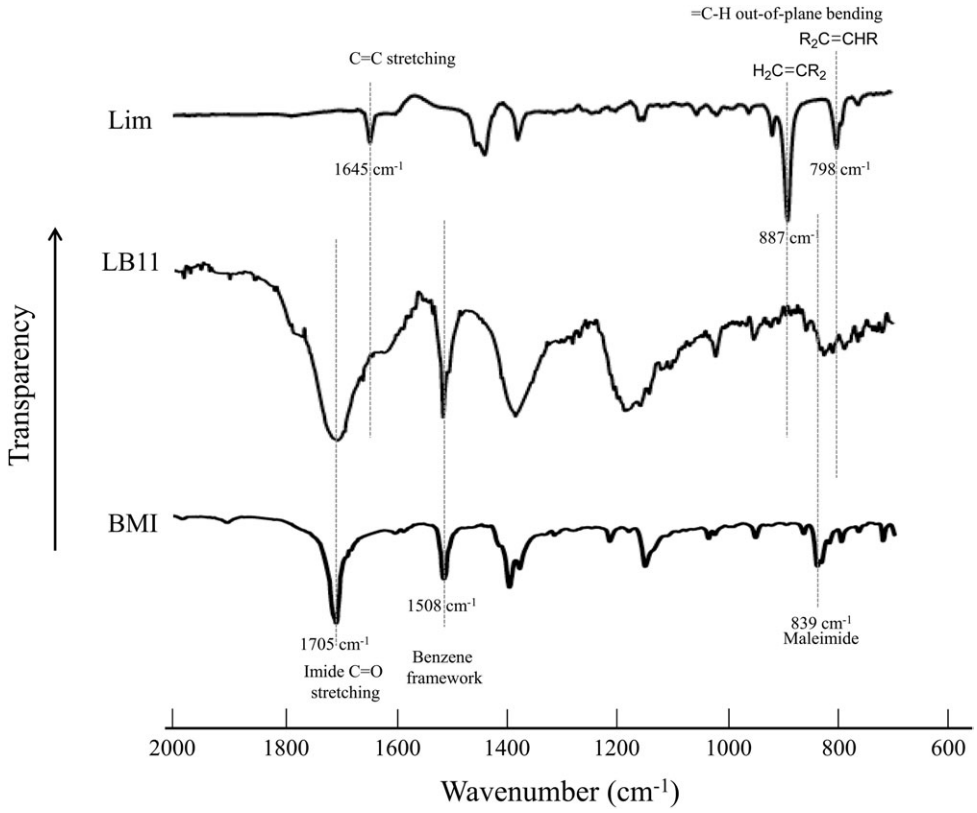

Figure 5. FTIR spectra of Lim, LB11, and BMI.

Applied Polymer SCIENCE

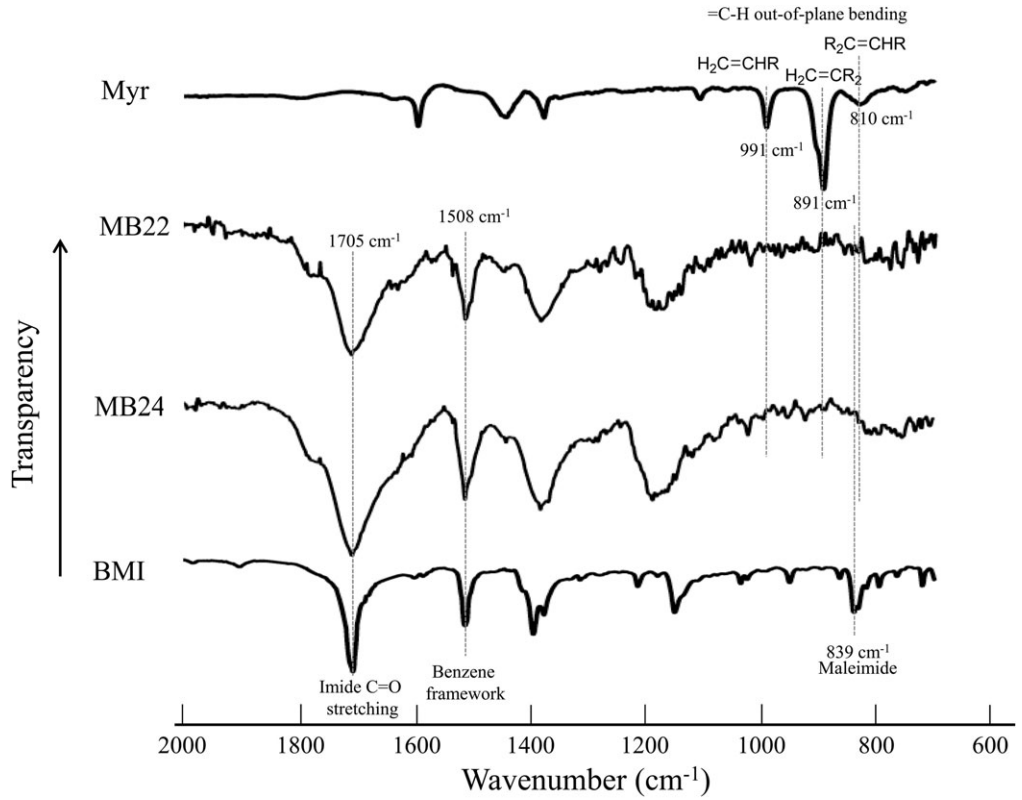

Figure 6. FTIR spectra of Myr, MB22, MB24, and BMI.

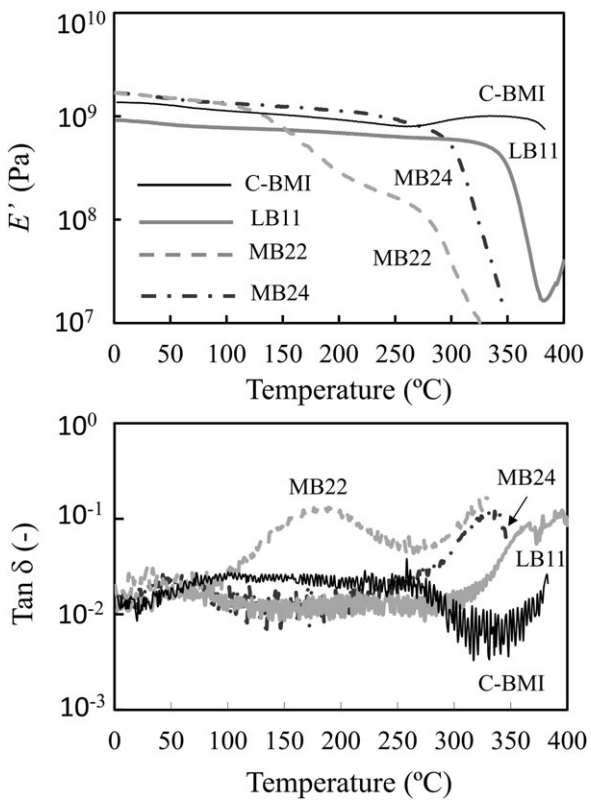

Figure 7. DMA curves of C-BMI, LB11, MB22, and MB24.

Figure 6 shows the FTIR spectra of MB22 and MB24 compared with those of Myr and BMI. Both the C—H out-of-plane bending absorption of the H_2C=CHR moiety of Myr at 991 cm^{-1} and that of the H_2C=CR_2 moiety of Myr at 891 cm^{-1} almost disappeared for MB22 and MB24, and new broad absorption peaks corresponding to the C—H out-of-plane bending absorptions of the formed cyclohexene R_2C=CRH moiety and *cis*-RHC=CHR moiety were observed around 860–700 cm^{-1}. These results indicate that the Diels–Alder and ene reactions of Myr and BMI occurred in a similar manner to the reactions of MP12 shown in Figure 4. The fact that the absorption peak related to the vinylidene H_2C=CR_2 out-of-plane bending absorption around 890 cm^{-1} was not clearly observed for MB22 and MB24 suggested that the vinyl copolymerization and/or ene reaction of the maleimide group and the vinylidene moiety

Table I. Thermal Properties of C-BMI, LB11, and the MBs

Sample	Tan δ peak temperature (°C)	10% weight loss temperature (°C)	Char yield at 590°C (%)
C-BMI	—	514.0	68.2
LB11	365	479.1	65.4
MB22	186	445.6	35.0
MB23	360	446.5	40.2
MB24	332	451.2	58.5
MB25	340	450.1	46.0

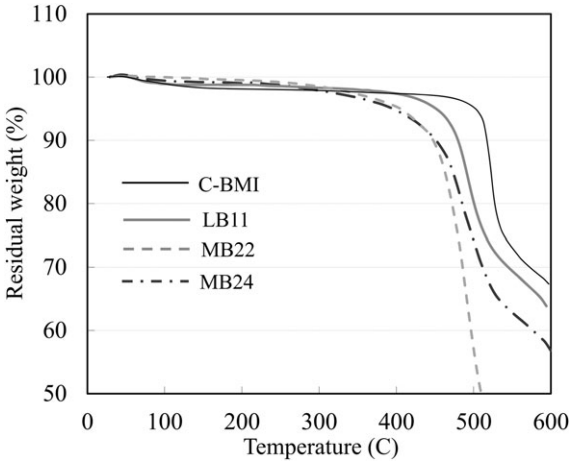

Figure 8. TGA curves of C-BMI, LB11, MB22, and MB24.

formed by the ene reaction, as shown in Figure 4, occurred further at the curing of Myr and BMI at 250°C. Also, most of the α,β-disubstituted olefin moiety formed by the ene reaction should have been *cis*-olefin (Figure 4) because there were little absorption peaks around 980–960 cm^{-1}, where the *trans*-RHC=CRH out-of-plane bending absorption peak should have been observed (MB22 and MB24 in Figure 6).[28] Similar reactions to the ene and Diels–Alder reactions for Lim/BMI and Myr/BMI have been reported for various alkenes and unsaturated carbonyl compounds in the literature.[20,29,30]

Properties of the Cured Resin of Terpene and BMI

Figure 7 shows the DMA curves of C-BMI, LB11, MB22, and MB24. The storage modulus (E') of C-BMI started to increase from about 250°C; this indicated that C-BMI was not fully cured at 250°C after 5 h. The E' value at a temperature lower than 100°C for MB22 and MB24 was higher than that for C-BMI. However, the E' value of LB11 was lower than that of C-BMI over the scanned temperature range. Table I summarizes the tan δ peak temperatures of C-BMI, LB11, MB22, MB23, and MB24. C-BMI did not show a clear tan δ peak until 350°C. MB22 showed a two-stage reduction of E' around 150 and 300°C. The tan δ peak temperature corresponding to the first stage was 186°C. If the Diels–Alder reaction and subsequent ene reaction ideally occurred for MB22, MB22 did not become a network polymer but rather a linear polymer. There was a possibility that MB22 contained some oligomeric compounds because of the insufficient progress of the ene reaction. All of the MBs and LB11 had low tan δ peak heights and broad tan δ peaks; this indicated that the fraction of the polymer chain relaxing at the glass-transition temperature was not so large and that a multiple-network structure or heterogeneous morphology was formed, respectively. LB11, MB23, MB24, and MB25 showed tan δ peak temperatures higher than 330°C; this suggested that the motion of the polymer chain was restricted until high temperatures were reached.

Figure 8 shows the TGA curves of C-BMI, LB11, MB22, and MB24. Table I also summarizes the values of the 10% weight loss temperature and char yield at 590°C as measured by TGA. All of the samples showed a 10% weight loss temperature higher than 440°C. The order of thermal degradation temperature was C-BMI > LB12 > MB′s. The fact that MB22 and MB23, with higher fractions of Diels–Alder adduct, had lower char yields suggested the occurrence of a retro-Diels–Alder reaction. LB11, with a higher fraction of vinyl copolymerization, showed the highest char yield among the terpene-containing cured resins.

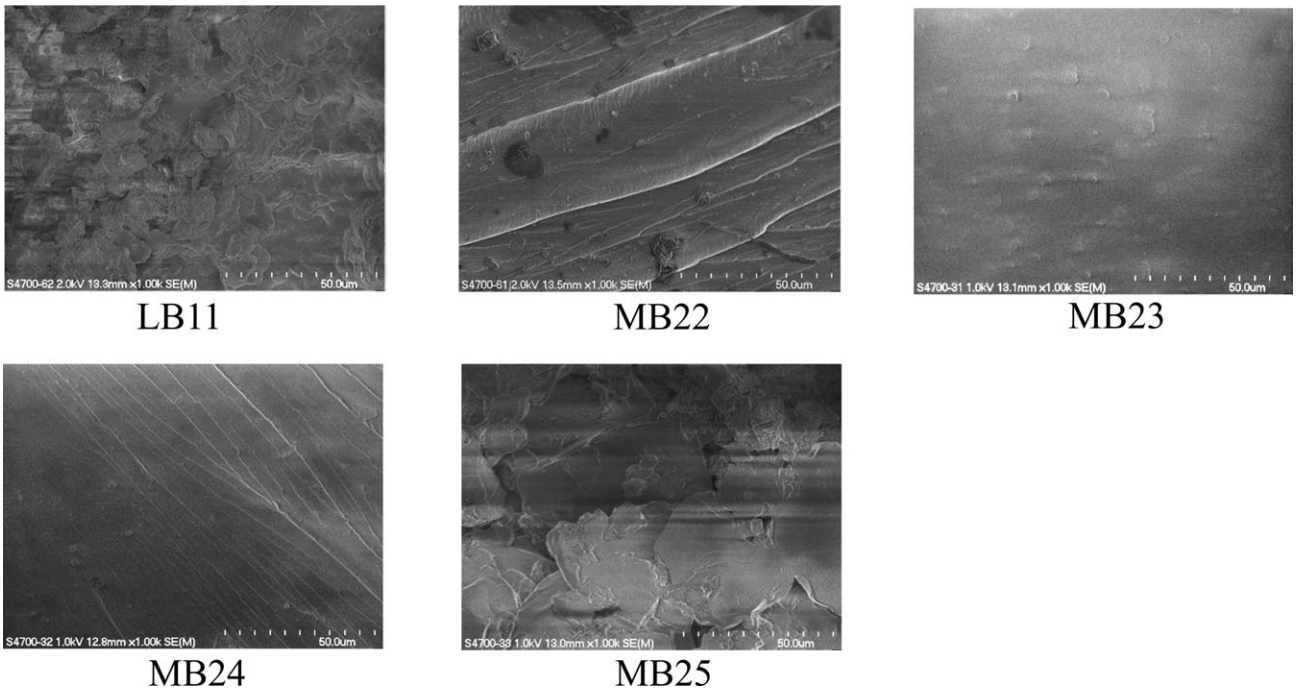

Figure 9. FE-SEM images of LB11, MB22, MB23, MB24, and MB25.

Figure 9 shows the FE-SEM images of the fracture surfaces of LB11 and the MBs. Although MB22, MB23, and MB24 had a homogeneous surface, some combined particles appeared for LB11 and MB25. This suggested that the Lim/BMI 1:1 prepolymer particles were not sufficiently unified by compression molding at 250°C because the prepolymer should have had a high molecular weight already because of the chain copolymerization at 150°C. This result was related to the fact that LB11 showed a lower E' than the MBs did. The heterogeneous morphology for MB25 indicated that excess BMI was homopolymerized and phase-separated.

Figure 10 shows the flexural properties of C-BMI, LB11, and the MBs. The flexural strength and modulus values of the MBs were higher than those of LB11 and C-BMI; this was in agreement with the morphological results of FE-SEM. MB22 and MB24 had the highest flexural strength and modulus, respectively, among the MBs. In general, the flexibility decreased and the rigidity increased with increasing BMI content. The fact that MB25 showed a lower flexural modulus was attributed to the heterogeneous morphology, as shown in Figure 9.

Hydrocarbon-modified BMI resins are expected to have water-resistance properties, which are especially required for electric materials. Figure 11 shows the water absorption values after 24 h for C-BMI, LB11, and the MBs. MB22, with the highest terpene content, had the lowest water absorption. However, LB11, which had the same terpene content as MB22, showed the highest water absorption. This result was attributed to the water permeation through microcracks caused by the insufficient combination of the prepolymerized particles of LB11. It is important in the preparation of compression-moldable thermosetting resins that stepwise Diels–Alder and ene reactions are preferred to chain radical polymerization.

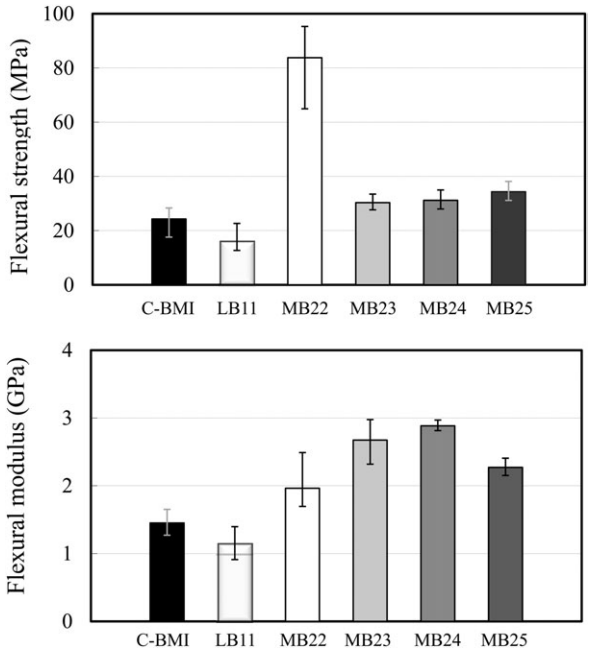

Figure 10. Flexural properties of C-BMI, LB11, MB22, MB23, MB24, and MB25.

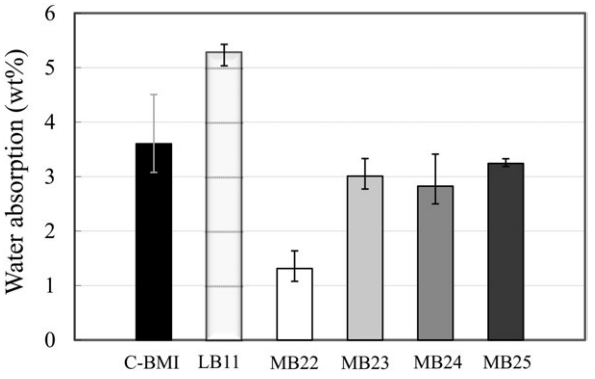

Figure 11. Water absorption of C-BMI, LB11, MB22, MB23, MB24, and MB25.

CONCLUSIONS

The prepolymers prepared by the precipitation of the reaction mixture of Lim and Myr with BMI in DMI at 150°C were compressed at 250°C, which produced LB11 and the MBs. Model reactions of Lim and Myr with PMI in DMI at 150°C were performed to evaluate the reaction mechanisms of LB11 and the MBs. The ^{1}H-NMR data revealed that the vinyl copolymerization for LP12 and the Diels–Alder reaction for MP12 preferentially proceeded in addition to the occurrence of ene reaction to some extent. The FTIR analysis of LB11 and the MBs supported the occurrence of their reactions. All of the cured resins, except for MB22, showed superior tan δ peaks and 10% weight loss temperatures. The flexural strength and modulus values of the MBs were higher than those of LB11 and C-BMI. The FE-SEM analysis revealed that MB22–MB24 were homogeneous, whereas some combined particles appeared for LB11. The MBs showed lower water absorption than C-BMI did.

ACKNOWLEDGMENT

The authors thank Naozumi Teramoto at the Department of Life and Environmental Sciences, Chiba Institute of Technology, for helpful suggestions and for measuring the ^{1}H-NMR spectra. They also thank Ryusuke Osada of the Material Analysis Center at Chiba Institute of Technology for assistance in measuring FE-SEM.

REFERENCES

1. Kaplan, D. L. In Biopolymers from Renewable Resources; Kaplan, D. L., Ed.; Springer-Verlag: Berlin, **1998**; Chapter 1, p 1.
2. Saheb, D. N.; Jog, J. P. *Adv. Polym. Technol.* **1999**, *18*, 351.
3. Bledzki, A. K.; Gassan, J. *Prog. Polym. Sci.* **1999**, *24*, 221.
4. Mohanty, A. K.; Misra, M.; Hinrichsen, G. *Macromol. Mater. Eng.* **2000**, *276/277*, 1.
5. Mohanty, A. K.; Misra, M.; Drzal, L. T. *J. Polym. Environ.* **2002**, *10*, 19.
6. Yu, L.; Dean, K.; Li, L. *Prog. Polym. Sci.* **2006**, *31*, 576.
7. Yu, L.; Petinakis, S.; Dean, K.; Bilyk, A.; Wu, D. *Macromol. Symp.* **2007**, *249/250*, 535.

8. Erickson, B.; Nelson, J. E.; Winters, P. *Biotechnol. J.* **2012**, *7*, 176.
9. Fitzpatrick, M.; Champagne, P.; Cunningham, M. F.; Whitney, R. A. *Bioresour. Technol.* **2010**, *101*, 8915.
10. Cherubini, F.; Ulgiati, S. *Appl. Energy* **2010**, *87*, 47.
11. Raquez, J. M.; Deléglise, M.; Lacrampe, M. F.; Krawczak, P. *Prog. Polym. Sci.* **2010**, *35*, 487.
12. Nair, C. P. R. *Prog. Polym. Sci.* **2004**, *29*, 401.
13. Hopewell, J. L.; George, G. A.; Hill, D. J. T. *Polymer* **2000**, *41*, 8221.
14. King, J. J.; Chaudhari, M.; Zahir, S. *29th SAMPE Symp.* **1984**, *29*, 392.
15. Morgan, R. J.; Shin, E. E.; Rosenberg, B.; Jurek, A. *Polymer* **1997**, *38*, 639.
16. Rozenberg, B. A.; Dzhavadyan, E. A.; Morgan, R.; Shin, E. *Polym. Adv. Technol.* **2002**, *13*, 837.
17. Hirayama, K.; Irie, T.; Teramoto, N.; Shibata, M. *J. Appl. Polym. Sci.* **2009**, *114*, 1033.
18. Shibata, M.; Teramoto, N.; Nakamura, Y. *J. Appl. Polym. Sci.* **2011**, *119*, 896.
19. Schewe, H.; Mirata, M. A.; Holtmann, D.; Schrader, J. *Process Biochem.* **2011**, *46*, 1885.
20. Yin, D. H.; Yin, D. L.; Fu, Z.; Li, Q. *J. Mol. Catal. A* **1999**, *148*, 87.
21. Veselovsky, V. V.; Gibin, A. S.; Lozanova, A. V. *Tetrahedron Lett.* **1988**, *19*, 175.
22. Kogami, K.; Takahashi, O.; Kumanotani, J. *Can. J. Chem.* **1974**, *125*, 125.
23. Solich, J. M.; Kupka, T.; Kluczka, M.; Solich, A. *Macromol. Chem. Phys.* **1994**, *195*, 1843.
24. Satoh, K.; Matsuda, M.; Nagai, K.; Kamigaito, M. *J. Am. Chem. Soc.* **2010**, *132*, 10003.
25. Parker, D. W. (Union Camp Corp.). U.S. Pat. 4,975,503 (**1990**).
26. Bruchmann, B.; Mijolovic, D.; Lange, A.; Stumbe, J. F.; Schonfelder, D.; Eipper, A. (to BASF Aktingesellschaft.). U.S. Pat. 2008/0312384 A1 (**2008**).
27. Gonçalves, J. A.; Silva, M. J.; Pilo-Veloso, D.; Howarth, O. W.; Gusevskaya, E. V. *J. Organomet. Chem.* **2005**, *690*, 2996.
28. Silverstein, R. M.; Webster, F. X.; Kiemle, D. J. In Spectrometric Identification of Organic Compounds, 7th ed.; Wiley: Hoboken, **2005**; Chapter 2, p 125.
29. Snider, B. B. *Compr. Org. Synth.* **1991**, *5*, 1.
30. Desimoni, G.; Faita, G.; Righetti, R. *Tetrahedron Lett.* **1995**, *36*, 2855.